Fracture 1977, Volume 1, ICF4, Waterloo, Canada, June 19 - 24, 1977

SOME ASPECTS OF FATIGUE CRACK GROWTH IN METALS AND ALLOYS

C. J. Beevers*

ABSTRACT

The fatigue crack growth (fcg) characteristics of metal and alloys are examined in terms of the influence of load ratio, microstructure and gaseous environments. The low fcg region which leads to thresholds is considered and the factors influencing ΔK and K_{max} control of this region discussed. The occurrence of microstructure sensitive fatigue crack growth and the formation of crystallographic facets in a wide range of materials and testing conditions is reported in detail. The intermediate fcg region where linear log ΔK v log da/dN curves are normally observed and fcg is relatively insensitive to mechanical properties is considered. Results for steels and titanium alloys tested in the intermediate to high fcg regions illustrate the influence of microstructure and environment on the form of the fcg curves. In general the theme of this paper is to illustrate the interplay between the ΔK and K_{max} controlled crack extension processes and how these influence the form of the fcg curves.

INTRODUCTION

Fatigue or repeated loading of materials is a subject with many facets. The response to loading is in many instances related to the pattern of the loading/environmental/microstructural profile. This profile may include such variables as loading sequence, load ratio, environment, microstructure, grain size, thermal activation, crack closure and dwell phenomena. The areas of specific interest to be considered in this paper are low fatigue crack growth (fcg) rates with some involvement in thresholds and crack closure. Secondly the intermediate fcg rate region where the crack growth rate da/dN can be readily related to the stress intensity range ΔK by equation (1).

$$\frac{da}{dN} = B.\Delta K^{m} \qquad (1)$$

The fast or higher fcg rate region where dwell effects can have a substantial influence will also be considered. These three regions of fcg are identified as A-low, B intermediate and C high in Figure 1. The conventional representation of fcg data in terms of da/dN and ΔK as shown in Figure 1. In many instances the magnitude of K_{max} can influence fcg behaviour and some consideration will be given to the origins of this K_{max} control and to identifying those situations where K_{max} can make an important contribution to the crack growth process.

*Department of Physical Metallurgy and Science of Materials, University of Birmingham, P.O. Box 363, Birmingham, B15 2TT, U.K.

LOW FATIGUE CRACK GROWTH RATES

This mode of fcg is identified as being in the region A of Figure 1. Characteristically, the upper level of ΔK is between 10 and 20 MPa$\cdot$m$^{1/2}$ and da/dN < 10^{-5} mm/cycle. In all instances the power exponent m in equation (1) is observed to increase with decreasing values of ΔK and da/dN. The form of the growth rate curve has been shown to be dependent upon R ratio (K_{min}/K_{max}), microstructure, environment, load history and the interaction of these variables.

The influence of R ratio on the form of the fcg curves is illustarted in Figure 2 for the case of a C/Mn pearlite steel [1]. The form of R dependence is observed in many metals and alloys including aluminium alloys [2], low carbon steels [3] pearlitic steels [4,5], quenched and tempered steels [6], α-titanium [7], and α/β titanium alloys [8,9]. It is clear from Figure 2 that at da/dN levels less than 10^{-5}mm/cycle fcg is sustained to lower ΔK levels as the K_{max} component is raised, that is for higher R values. The deviation from linearity of the fcg curves has been associated with the occurrence of *microstructural sensitive* fatigue crack growth. This mode of fcg can manifest itself as planar transgranular facets or as intergranular facets. In α-titanium and α/β titanium alloys the facets are transgranualr. An example of such facets is shown in Figure 3. The size of the facetted region was the same size as the α grain size in both materials. The development of the facets as a function of ΔK is shown in Figure 4. The corresponding fcg curve is shown in Figure 5. The development of the facets was associated with the change from microstructural insensitive to microstructural sensitive crack growth and a transition from mode B to A (Figure 5). The separation at the crack front of the material which did not facet involved a ductile tearing process. In titanium alloys it has been demonstrated by spiking the loading sequence [10] that facets form as a result of continued load cycling and are not "cleavage" facets. In quenched and tempered steels and low plain carbon steels [11] microstructural sensitive fcg involves intergranualr modes of separation. Figure 6 shows an SEM photograph of a fracture surface taken from an 0.01% C, 0.85% Mn steel tested in laboratory air (RH > 90%) at R = 0.35 and at a frequency of ~ 100 Hz. The fracture surface morphology is characteristic for separation at $\Delta K \sim 10$ Mpa$\cdot$m$^{1/2}$ and da/dN ~ 10^{-6} mm/cycle. In quenched and tempered low alloy steels intergranular separation is observed in both low and high fcg rate regions. Figure 7 shows the percentage of fracture surface consisting of intergranular facets for an En 24 steel given the following heat treatment. One and a half hours at 1250^{0}C oil quenched, 625^{0}C for one hour, air cooled followed by 480^{0}C for four hours and air cooled. The prior austenite grain size was ~ 88 μm and yield stress 1090 MPa. The intergranular facetting can be seen to develop strongly over the ΔK range 25 to 14 and then diminish. This development and subsequent decrease in facetting has been observed in En 24 after varying tempering treatments [6,12]. The fcg curves become R sensitive over the same ΔK range that the facetting develops [6]. An example of the intergranular facetting with the accompanying ductile tearing is shown in Figure 8.

This occurrence of microstructural sensitive crack growth has been related [6-9, 13] to a grain size/crack tip plasticity interaction. Specifically the occurrence of both trans and intergranular facets has been shown to occur when the reverse plastic zone size P_r as defined in equation (2) is of a smaller size to the grain size [6-9].

$$P_r = \frac{1}{3\pi}\left(\frac{\Delta K}{2\sigma_y}\right)^2 \qquad (2)$$

In 316 stainless steel transgranular facet formation increases over the ΔK range 30 to 15 and then decreases to zero at ΔK = 5 Mpa$\cdot$m$^{1/2}$ [14]. The percentage area of fracture surface covered by facets was small, 10% or less, compared with the α/β titanium and the alloy steels. The ΔK for peak facet formation and percentage of area covered by facets increased with grain size. This observation is consistent with the views proposed earlier.

Some information concerning transgranular facet formation is presented in Table 1. The planes are usually near close packed planes of the parent lattice i.e. {001} in the fcc and {0001} in the cph lattice. Most authors reported the use of Laué or microbeam Laué X-ray back reflection techniques for facet plane orientation. The use of SACP (Selected Area Channelling Patterns) on the SEM [26] is proving auseful technique as a working spot size of 100 μm can be readily achieved. An example of a facet on the fatigue fracture surface of α-titanium identified as an (0001) plane is shown in Figure 9. The models proposed for the formation of facets involves alternating slip activity i.e. {111} slip leading to {001} planes of separation in aluminium and copper [23,28]. When the reverse plasticity at the crack tip is contained within individual grains then the anisotropy of slip activity will produce a facet whose plane will be determined by the orientation of the grain with respect to the principal stress. In a polycrystalline material with a random grain orientation one should expect to find facets of varying orientation to the macroscopic crack plane. This is indeed observed [7] and a characteristic of A mode growth in many materials is that the fatigue fracture surface is roughened in comparison to the smoother fracture faces from mode B.

Environment is an important factor and intimately linked into the formation of microstructural sensitive fcg. In α-titanium, α/β titanium, plain low carbon steels and quenched and tempered steels the trans and intergranular facetting is not observed on the fatigue fracture surfaces if the materials are tested in vacuum (~10^{-5}torr or 1.33 mN m^{-2}). At the same time the R dependence of the fcg curves is much reduced. For transgranularly facetted material the fcg curves in vacuum (dotted line in Figure 1) are held at higher ΔK levels and the fcg rates are slower than in laboratory air. (Figure 5). The lack of R dependence of the fcg curves in vacuum reinforces the view that in some way the occurrence of facet formation and the development of a K_{max} dependence of the fcg curves are linked. A model to explain this behaviour [7] was produced as a result of work on α-titanium where it was observed that facetting and an increase in grain size resulted in lower fcg rates. This observation has been supported by results obtained from a low carbon steel where an increase in grain size resulted in lower fcg rates [29]. The model involves a bimodal form of crack growth in which one component is ΔK dependent and the other K_{max} dependent. For low R values a strong K_{max} dependence would be expected whilst at high R values a ΔK dominance of the fcg curves could be expected. The form of the ΔK - K_{max} interaction would be dependent upon both microstructure and environment. The quantitative influence of these parameters on the fcg curves is yet to be resolved.

THRESHOLDS

From the form of the da/dN v ΔK vurves in Region A (Figure 1) the fcg rates decrease rapidly for small decrements of ΔK. The implication of this behaviour is that the cruves will approach asymtotically a ΔK threshold. In practice ΔK_{th} as a stress intensity below which crack

growth does not occur is not evaluated. The values quoted for ΔK_{th} in most instances are those ΔK values which result in a fcg rate in the range 10^{-6} to 10^{-8}mm/cycle. Extrapolation of fcg curves to low da/dN values to obtain ΔK_{th} has the obvious disadvantage that it presumes the form of the fcg curves. It is also important to recognize the influence of stress history and the necessity of careful step down procedures to avoid ambiguous observations.

Most thresholds have been measured in laboratory air, some in vacuum and aqueous environments and most at frequencies of 50 to 100 Hz or greater. The values of these tresholds have been reported by Pook [30] and Wiess and Lal [31]. The general trends show that the threshold ΔK levels for many materials in air are R ratio sensitive, that is ΔK_{th} tends to decrease with increasing R but for R > 0.5 the sensitivity is much reduced. This observation is consistent with the ΔK - K_{max} interaction outlined in the previous section. The relative influence of ΔK and K_{max} on the threshold level can be considered in terms of the γ value in equation (3)

$$\Delta K_{th} = K_{thD} (1 - R)^{\gamma} \tag{3}$$

Many materials tested in laboratory air exhibit a γ value in the region of 0.5 with the mild steels and pearlitic steels having somewhat higher values in the region 0.7 to 0.9. The variation of ΔK_{th} with R for three nominally high strength aluminum alloys is presented in Figure 10. Associated with the threshold regions which involved growth rates of less than 10^{-8}mm/cycle were smooth flat regions relatively insensitive to the microstructure (Figure 11). The value of γ for these aluminium alloys is 1.0, that is the thresholds occurred at a constant K_{max}.

The results in Table II for a range of materials show that γ is influenced by the presence or otherwise of laboratory air. There is no influence of K_{max} on the threshold levels in low alloy steels and titanium alloys when tested in vacuum [6,8]. Some recent work by Lindley [32] however on a 13% Cr steel indicates a possible R dependence in vacuum of ΔK_{th}.

Microstructural variables also influence the threshold level for α/β titanium alloys tested in air, a higher threshold level for β heat treated material was observed [10]. Extensive crack branching was associated with those microstructures exhibiting a higher threshold. A further influence on threshold level can be grain size. Tests on an 0.07% C, 0.46% Mn steel have shown that the threshold is dependent upon grain size and that the threshold ΔK level increases with grain size as shown in equation (4).

$$\Delta K_{thD} = 3.8 + 1.4 \times 10^{3}\, d^{1/2} \tag{4}$$

where d is the grain size in metres. The yield stress decreased with the increased grain size according to the relationship in equation (5).

$$\sigma_y = 139 + 0.347\, d^{-1/2} \tag{5}$$

The influence of grain size on fcg in α-titanium [7] also indicates higher thresholds with larger grain sizes. This effect of grain size on thresholds is the reverse of that on fatigue limits. In both titanium alloys [33] and steels [34] the fatigue limit is raised by a decreasing grain size. This emphasises the basic difference in the physical character of thresholds and fatigue limits. Nominally, the fatigue limit is concerned with the probability of initiation of cracks and the development

to a condition where sustained growth may take place. On the other hand thresholds as measured are the condition for crack arrest not initiation. In a series of pearlitic and pearlitic/martensitic steels [4], the threshold stress was observed to occur at constant value of the maximum plastic zone size as defined by equation (6).

$$P_m = \frac{1}{3\pi} \left(\frac{K_{max}}{\sigma_y} \right)^2 \tag{6}$$

There have been several models proposed to explain the "threshold" phenomena. Pook [30] suggested that cracks cannot grow at a rate less than one interatomic spacing per load cycle. It has been suggested that the threshold condition for non-propagating cracks in aluminium, copper and magnesium alloys can be described by an expression of the form shown in equation (7).

$$\Delta K_{th} = AE - B\sigma_y \tag{7}$$

Klesnil and Lukas [35,36] have studied the threshold behaviour in a series of steels and emphasized the importance of stress history. They consider that the R dependence of the threshold can be explained in terms of the compressive stresses which result from the formation of the plastic zone at the crack tip. Schmidt and Paris [37] have proposed a physical explanation for thresholds and R value effects in terms of crack closure concepts. Tests on α-titanium in the ΔK range 3 to 12 MN $m^{-3/2}$ have shown that K_o, the stress intensity for fill crack face separation was greater than K_{min} and K_o was closely linked to K_{max}. For a series of tests involving different load sequences and load ratios the log (K_{max} - K_o) v log da/dN plots showed a much closer correlation than the log ΔK v log da/dN plots. These observations [38] show that fatigue crack closure can be important in the low fcg regions but do not show that closure is necessarily the controlling factor for thresholds. Weiss and Lal [31] have developed the expression shown in equation (8).

$$K_{th}^{\,2} = \frac{3\pi}{2} (0.1\, E)^2\, \rho^* \tag{8}$$

For a conservative value of ΔK ρ^* = 250 x 10^{-10}m is recommended.

The influence of elastic modulus on threshold levels is evident in the general magnitude of the threshold stress for different metals and alloys. However, microstructural and grain size effects can alter the threshold level significantly for the same material. The presence of laboratory air compared to an inert atmosphere also influences the threshold level. The structural features on the fracture face at threshold are difficult to establish but the facetting of both a trans and intergranular character is not obvious at these lower ΔK levels. In view of the difference in the control of threshold levels in air and vacuum some distinct differences in fracture surface morphology might be expected. In vacuum $\gamma \sim 0$ and the ΔK_{th} is insensitive to changes in R whilst in air for some materials $K_{max(th)}$ is more appropriate than ΔK_{th}. The K_{max} dependence of the threshold might be expected to be influenced by the rate of access to the crack tip of the environment and thus be influenced by partial vapour pressures and frequency of loading. It is clear that predicting unique values for the threshold is extremely difficult and that a threshold range or $\overline{\Delta K_{th}}$ should be used to incorporate variables such as microstructure, environment, frequency and closure.

INTERMEDIATE FATIGUE CRACK GROWTH RATES

Following the initial proposal of Paris and Erdogan [41] many metals and alloys have been shown to exhibit fcg characteristics which can be described by equation (1) over a limited ΔK range. Several authors [42-44] have shown that the reverse plasticity at the crack tip is the important factor controlling the process of crack tip extension. The consequence of this reversed plastic flow at the crack tip manifests itself in some materials by the formation of striations on the fatigue fracture surface. An example of this type of fracture surface morphology is shown in Figure 12. The influence of microstructural and mechanical properties on this stage of fcg are well documented [45,46]. The following results and discussion therefore are focussed in the direction of load ratio and environmental influences on intermediate fcg rates.

The aluminium alloys which were investigated to provide the threshold data in Figure 10 were also tested to higher ΔK levels and the fcg curves for alloy 7075 T651 are presented in Figure 13. The results were obtained from 10 mm thick samples tested in wet air (Relative Humidity > 90%) and dry air (Relative Humidity ~ 35%) at R ratios of 0.07, 0.35 and 0.70. Over the whole ΔK range examined the effect of increasing R and the relative humidity was to raise the fcg rate. The rate was increased for the mid-ΔK range by as much as 20 times. The 7075 T7351 showed a similar effect but for the aluminium-copper alloy 2L93 the effect was somewhat reduced. A comparison of the three alloys tested in wet air at R = 0.07, 0.35 and 0.70 can be obtained from the results presented in Figure 14. The tensile properties of the three alloys are presented in Table III. At the high R ratios the fully hardened Al/Zn/Mg alloy exhibited the faster fcg rates but at the low R ratio there was little difference in the behaviour of the three alloys. S.E.M. observations of the fracture surfaces showed the following trends. At low ΔK's facet formation was observed and this diminished with increasing ΔK to be replaced by striation formation and ductile tearing, some brittle striations were also observed. An example of this ductile tearing is shown in Figure 15. The ductile tearing mode was observed in a qualitative manner to be more prevalent on the fracture surfaces of the high R and wet air tests. These observations are in general agreement with previous observations of fracture surfaces of fatigued aluminium alloys [15,16,18,47,48]. These results demonstrate the influence of load ratio and environment and their combined influences that they can have on fcg rates in aluminium alloys. A consequence of these results is that a separation process in which K_{max} is important as well as ΔK can occur over almost the entire range of low and intermediate fcg range. (Regions A and B in Figure 1).

The specific mechanisms whereby "environmental" effects occur are difficult to elucidate. The subject has sustained interest for some considerable time. In 1932 Gough and Sopwith [49] reported that fcg rates could be reduced by cycling in vacuum rather than air. Thompson [50] suggested that the improved fatigue life in vacuum may be due to a degree of welding taking place at the crack tip. This view has not received general support and attention has been given to the probable role of the different constituents of laboratory air. For example Wadsworth [51] showed that a vacuum of 7×10^{-6} torr gave a reduction by a factor of 20 in the fatigue life of copper. For aluminium the water vapour content of the air appeared to be the controlling influence. Bradshaw and Wheeler [2] carried out a series of tests comparing various constituents with vacuum. They found that whilst moist air increased the fcg dry argon and dry hydrogen had little effect. Later the same authors [52] showed that the critical

vapour pressure of the water vapour P_{crit} to influence fcg rates was given by equation (8).

$$P_{crit}\ (Pa) = 4 \times 10^{4}\ [\text{Frequency Hz} \times \text{fcg rate mm/cycle}] \qquad (9)$$

Brown and Nicholson [53] suggested that the release of hydrogen as a result of the reaction of water vapour with the crack tip was an important factor influencing fcg rates. Meyn [18] found the fcg rates of aluminium in air to be three times the rate in vacuum. In vacuum no striations were formed on the fatigue fracture surface. Facets were formed in vacuum as well as air in coarse grained (~4 mm) samples. Two types of facets, those associated with {001} planes and shiny faces identified as {111} planes were observed. Other workers [21] have reported the formation of rippled facets during fcg in aluminium in air and distilled water. Meyn [22] reported environmental effects in α/β titanium alloys and related these to a cyclic loading/stress corrosion interaction. The ratio of fcg rates in air as compared to an inert environment increased as the stress amplitude decreased.

There have been many investigations concerned with identifying the particular species responsible for increased fcg rates [54-60]. Water vapour, hydrogen and oxygen have all been proposed as the major embrittling species. There is no rule as to which species embrittles which material. This situation is further complicated by the interaction of changes in load ratio, microstructure and frequency with the active species. The embrittling mechanism may involve surface reactions or require diffusion to the material ahead of the crack tip. The diffusion of hydrogen or oxygen to a region of strongly dilated lattice just ahead of the crack tip and the possible effects upon the work to create new surfaces is an area which should yield interesting conclusions.

HIGH FATIGUE CRACK GROWTH RATES

The sigmoidal form of the log da/dN v log ΔK plot shown in Figure 1 indicates that there is an acceleration of the fcg rate in Region C and that this mode of growth can be initiated at lower ΔK values for higher levels of R ratio. This involvement of the K_{max} component in the fcg process would be expected as K_{max} approaches K_C. The influence of microstructure, environment and load ratio on the behaviour of several different materials will be examined in this section of the paper.

The influence of microstructure on the behaviour of a C/Mn pearlitic steel is illustrated in Figure 16 [1]. The material MP was an 0.55% C 2.23% Mn steel with a 95% fine pearlite 5% banded martensite microstructure. The results over a similar ΔK range and R ratios for an 0.55% C 0.6% Mn steel were presented in Figure 2. Comparison of the two plots shows that the steel MP exhibited the form of fcg curve in which the intermediate stage B (Figure 1) is extremely limited in range. This narrow K range for the intermediate fcg region B is primarily a consequence of an initiation of region C at lower ΔK levels in steel MP. An S.E.M. examination of these steels revealed the presence of extensive cleavage on the fatigue fracture faces. An example of these cleavage fracture regions is shown in Figure 17. A quantitative S.E.M. study revealed that percentage area of fracture surface covered by cleavage fracture increased substantially between a K_{max} of 15 and 20 and this K_{max} value was independent of R ratio.

A coarse grained, low carbon, high nitrogen steel was tested over the ΔK range 15 to 40 and at R ratios 0.05 to 0.5 [1]. Cleavage fracture was observed on the fatigue fracture surfaces as in the case of the pearlitic steel. Quantitative metallographic examination of the fracture surfaces revealed that the % of fracture face covered by cleavage increased rapidly in K_{max} range 20 to 30 and was independent of R ratio. The build up of cleaved areas on the fracture face was initiated in the pearlitic steel at lower K_{max} levels than in the plain carbon steel. Both materials are examples of the influence of sub-critical cleavage on the fcg characteristics. It was concluded [1] that the strong R dependence of the fcg curves (Figure 16) is a consequence of the occurrence of the K_{max} dominated cleavage process. The influence on the fcg curves was most striking in the pearlitic steels and was related to the presence of banded martensite. Detailed metallographic studies indicated that cleavage in many instances was initiated from the pearlite/martensite platelet interfaces. The acceleration of the fcg rates was considered to have occurred as a result of the linkage of independently initiated subcritical cleavage cracks.

A strong R ratio dependence of the fcg curves of an α/β titanium alloy (Ti 6AL 4V) can be observed in the results presented in Figure 18. The tests were carried out in laboratory air and in vacuum (~ 0.7 mPa). The tests were carried out R ratios of 0.7, 0.55, 0.35 and 0.25 at a frequency of 0.2 Hz. For K's greater than ~ 20 Mpa$\cdot$m$^{1/2}$ a strong influence of K_{max} is evident in both air and vacuum. In all cases the rate of fcg for a particular ΔK level was less in vacuum than air. The similar in character to the naked eye. From S.E.M. observations it was noted that striation formation occurred readily on the fracture faces of specimens tested in air except for the high R test. The striation spacing could be readily linked with the growth/cycle as established from optical and potential drop methods. The fracture surfaces from the vacuum tests did not reveal the presence of striations as readily as in the case of the air tests. Other features of the fracture surface included some facets at the lower ΔK values and a build up of ductile voids or dimples at the higher K_{max} levels. An example of mixed mode growth with striations and ductile tearing is presented in Figure 17. In this material the fracture mode which was K_{max} dominated and lead to the strong R dependence of the fcg curves was separation by ductile tearing. This can be compared with the steels [1] where the R dependence comes mainly from sub-critical cleavage crack formation.

A further sharpening of the R ratio effect in the α/β titanium alloy was observed when dwell times of 10 minutes at the maximum load of the load cycle were introduced. In both air and vacuum tests the fcg rates were increased by a factor of 10 to 50 over a limited ΔK range. This effect was predominantly a feature which occurred when K_{max} was greater than ~ 40 MPa$\cdot$m$^{1/2}$. Sustained load cracking experiments in air showed that 40 Mpa$\cdot$m$^{1/2}$ was also the K_{max} level below which static crack growth rate was diminishingly small. Examination of the material ahead of the crack tip by careful metallographic sectioning showed that transgranular crack formation in the α-grains was associated with the acceleration of the fcg rate. S.E.M. observations of the fracture surfaces of dwell and sustained load specimens revealed the presence of facets. An example of the fracture face of a sustained load specimen is shown in Figure 20. Meyn [22] examined the fcg behaviour of a Ti 8Al 1Mo 1V alloy and showed that when K_{max} was greater than K_{ISCC} the fcg rate became sensitive to the frequency of the load cycle. The fracture surfaces also exhibited facet formation. The present results in many ways were consistent with the

earlier observations of Meyn [22].

The present observations show that a change in the fracture mode by allowing increased time for the influence of some species such as hydrogen to reach the crack tip and its vicinity can produce marked changes in the fcg rate. The specific facet planes were not identified in the present work. If, however, the orientations of the facets were of a constant character then texture would have to be also considered as a variable in the factors which can influence fcg rates.

The results presented in this section are like those reported by other authors [61,62] show that microstructure and environment can introduce a strong K_{max} element into the control of fatigue crack growth rates.

ACKNOWLEDGEMENTS

The author wishes to thank Professor R. E. Smallman for providing the facilities for the preparation of this report. The financial support of the Procurement Executive MOD, SRC and British Railways in the pursuance of the results presented in this paper is gratefully acknowledged.

REFERENCES

1. BEEVERS, CJ.J., COOKE, R.J., KNOTT, J.F. and RITCHIE, RO., Met. Sci. J., 9, 1975, 119.
2. BRADSHAW, J.F. and WHEELER, C., App. Mat. Res., 5, 1966, 112.
3. DRUCE, S.G., Private Communication.
4. COOKE, R.J. and BEEVERS, C.J., Mat. Sci. and Eng., 13, 1974, 210.
5. COOKE, R.J. and BEEVERS, C.J., Eng. Frac. Mech., 5, 1973, 1061.
6. COOKE, R.J., IRVING, P.E., BOOTH, G.S. and BEEVERS, C.J., Eng. Frac. Mech., 7, 1975, 69.
7. ROBINSON, J.L. and BEEVERS, C.J., Met. Sci. J., 7, 1973, 153.
8. IRVING, P.E. and BEEVERS, C.J., Met. Sci. and Eng., 14, 1974, 229.
9. IRVING, P.E. and BEEVERS, C.J., Met. Trans., 5, 1974, 391.
10. PATON, N.E., WILLIAMS, J.C., CHESNUT, J.C. and THOMPSON, A.W., AGARD Conference Proceedings No.185, "Alloy Design for Fatigue and Fracture Resistance".
11. DRUCE, S.G., Private Communication.
12. IRVING, P.E., Private Communication.
13. BIRKBECK, G., INKEL, A. and WALDRON, G.M., J. Mat. Sci., 6, 1971, 319.
14. PRIDDLE, E.K. and WALKER, F.E., J. Mat. Sci., 11, 1976, 386.
15. FORSYTH, P.J.E., STUBBINGTON, C.A. and CLARK, D., J. Int. Metals, 90, 1963, 238.
16. STUBBINGTON, C.A., Metallurgia, 68, 1963, 109.
17. WILLIAMS, H.D. and SMITH, G.C., Phil. Mag., 13, 1966, 835.
18. MEYN, D.A., Trans. ASM, 61, 1968, 52.
19. GELL, M. and LEVERANT, G.R., Acta Met., 16, 1968, 553.
20. THOMPSON, K.R.L. and CRAIG, J.V., Met. Trans., 1, 1970, 1042.
21. FEENEY, J., McMILLAN, J.C. and WEI, P.R., Met. Trans., 1, 1970, 1741.
22. MEYN, D.A., Met. Trans., 2, 1971, 853.
23. GARRETT, G.G. and KNOTT, J.F., Acta Met., 23, 1975, 841.
24. NEAL, D.E. and BLENKINSOP, P.A., Acta Met., 24, 1976, 59.
25. PRIDDLE, E.K. and WALKER, F.E., J. Mat. Sci., 11, 1976, 386.
26. WARD-CLOSE, C.M., Private Communication.
27. RICHARDS, C.E., Acta Met., 19, 1971, 583.

28. NEUMAN, P., Acta Met., 22, 1974, 1155.
29. MASOUAVE, J. and BAILON, J.P., Scripta Met., 10, 1976, 165.
30. POOK, L.P., ASTM STP, 513, 1972, 106.
31. WEISS, V. and LAL, D., Met Trans., 5, 1974, 1946.
32. LINDLEY, T., Private Communication.
33. LUCAS, J.J., Titanium Science and Technology, Plenum Press, N.Y., 3, 1973, 2081.
34. YOKOBORI, T. and KAWASHIMA, T., Rep. Res. Inst. Strength and Fracture of Materials, 5, 1969, 51.
35. KLESNIL, M. and LUKAS, P., Met. Sci. Eng., 9, 1972, 231.
36. KLESNIL, M. and LUKAS, P., Eng. Frac. Mech., 4, 1972, 77.
37. SCHMIDT, R.A. and PARIS, P.C., ASTM STP, 536, 1973, 79.
38. HERMAN, L. and BEEVERS, C.J., Brown University Report, 1976.
39. KIRBY, B., Private Communication.
40. HICKS, M., Private Communication.
41. PARIS, P.C. and ERDOGAN, F., J. Basic Eng., 85, 1963, 528.
42. TOMPKINS, B., Phil. Mag., 18, 1968, 1041.
43. LAIRD, C., ASTM STP, 415, 1967, 139.
44. PELLOUX, R.M.N., Eng. Frac. Mech., 1, 1970, 697.
45. PLUMBRIDGE, W.J., J. Mat. Sci., 7, 1972, 939.
46. TETLEMAN, A.S. and McEVILY, A.J., Fracture of Structural Mechanics, Wiley, N.Y., 1967.
47. FORSYTH, P.J.E. and RYDER, D.A., Metallurgia, 63, 1961, 117.
48. FORSYTH, P.J.E., Acta Met., 11, 1963, 703.
49. GOUGH, J. and SOPWITH, D.G., J. Inst. Met., 49, 1932, 93.
50. THOMPSON, N., WADSWORTH, N. and LOUAT, M.P., Phil. Mag., 1, 1956, 113.
51. WADSWORTH, N.J. and HUTCHINSON, J., Phil. Mag., 3, 1958, 1154.
52. BRADSHAW, F.J. and WHEELER, C., Int. J. Frac. Mechs., 5, 1969, 255.
53. BROOM, T. and NICHOLSON, A.J., Inst. Met., 89, 1960, 183.
54. SHAHINIAN, P., WATSON, H.E. and SMITH, H.A., J. of Materials, JMLSA, 7, 1972, 527.
55. FROST, N.E., App. Mat. Research, 3, 1964, 131.
56. STEGMAN, R.L. and SHAHINIAN, P., Met. Sci. J., 6, 1972, 123.
57. VAN SUAN, L.F., PELLOUX, R.M. and GRANT, N.H., Met. Trans., 6A, 1975, 45.
58. SPITZIG, W.A. and WEI, R.P., Eng. Frac. Mech., 1, 1970, 719.
59. SPITZIG, W.A., TRALDA, P.M. and WEI, P.R., Eng. Frac. Mech., 1, 1968, 155.
60. SPITZIG, W.A. and WEI, R.P., Trans. ASM, 60, 1967, 279.
61. RICHARDS, C.E. and LINDLEY, T.C., Eng. Frac. Mech., 4, 1972, 951.
62. RITCHIE, R. O. and KNOTT, J. F., Acta Met., 21, 1973, 639.

Table 1 Cystallographic facets formed during microstructural sensitive fcg.

Reference	Material	Environment	ΔK . $\frac{da}{dN}$. N_f	Facet Plane	Identification Technique
15	Al Zn Mg	Laboratory Air		{001}	Laué X-ray
16	Al Zn Mg	3% NaCl solution	10^3	{001}	Laué X-ray
17	Cu 47.6% Zn	Laboratory Air	10^5 ↓ 10^7	{110} ± 10^o	Laué X-ray
18	Al 2024	Laboratory Air	5.5 ↓ 16.5	3^o to 20^o from {100}	Laué X-ray
18	Al 2024	Vacuum (3×10^{-3} torr)	5.5 ↓ 16.5	{001} ± 5^o {111}	Laué X-ray
19	Nickel Superalloy	Laboratory Air	10^4 ↓ 10^7	{111}	Laué X-ray
20	Al 2219-T6	Laboratory Air		{111} ± 5^o	Laué X-ray
21	Al 2024 - 7075 7178	Dry Air Wet Air Distilled Water	2.2 ↓ 11.0		

Table 1 Continued

Reference	Material	Environment	ΔK . $\frac{da}{dN}$. N_f	Facet Plane	Identification Technique
22	Ti 8Al 1Mo 1V	3½% NaCl solution	1.1 ↓ 100	{0001} and 15^o from {0001}	Laué X-ray
22	Ti 8Al 1Mo 1V	Vacuum (2×10^{-7} torr)	1.1 ↓ 100	two {1120} examples	Laué X-ray
23	Al 3% Cu	Laboratory Air	7 ↓ 30	{001} ± 5-10^o	Laué X-ray
24	Ti 6Al 4V Ti 4Al 4Mo 2Sn 0.5Si	Dry Air Moist Air	10^7	15^o from (0001) {10$\bar{1}$7}	Laué X-ray
25	316 Stainless Steel	Laboratory Air	5.5 ↓ 30.0	{111}	X-ray
26	α-Titanium 155	Laboratory Air	5 ↓ 14	(0001) ± 5^o	SACP, Selected Area Channelling Pattern
27	Fe 3%Si	Laboratory Air	10 ↓ 30	{001}	

Table 2 The values of γ (equation 3) obtained from a range of materials and testing conditions ΔK_{th} obtained from fcg rates at $\sim 10^{-8}$ mm/cycle.

Reference	Material	Environment	γ
39	Aluminium Alloys	Laboratory Air	1.0
35, 36	Steels	Laboratory Air	0.71
5	Pearlitic Steels	Laboratory Air	0.93 0.94
6	En 24 Steel	Laboratory Air	0.47
		Vacuum	0.0
12	En 24 Steel	Laboratory Air	0.17
		Vacuum	0.0
9	Ti 6Al 4V	Vacuum	0.0
40	Ti Alloy	Laboratory Air	0.7

Table 3 The mechanical properties of the aluminium alloys in Figures 13 and 14

Alloy	0.2% P.S. MPa	U.T.S. MPa	% elongation to fracture
2L93	425	456	7
7075 - T651	490	548	9
7075 - T7351	412	488	10

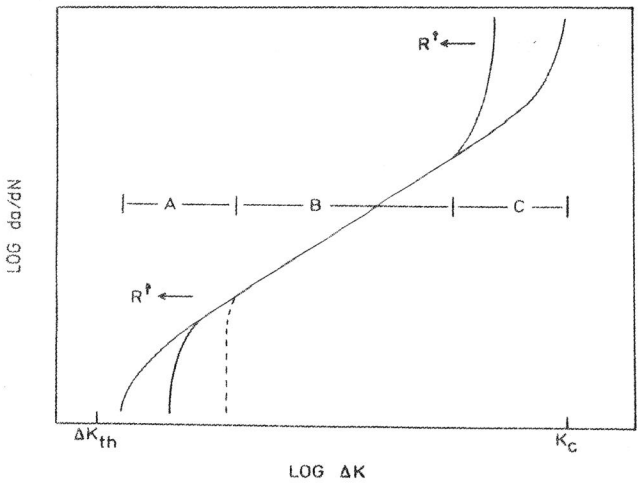

Figure 1 A schematic representation of the sigmoidal log da/dN v log ΔK curve developed by many metals and alloys. Region A low fatigue crack growth rates. Region B intermediate fatigue crack growth rates and C, high fatigue crack growth rates.

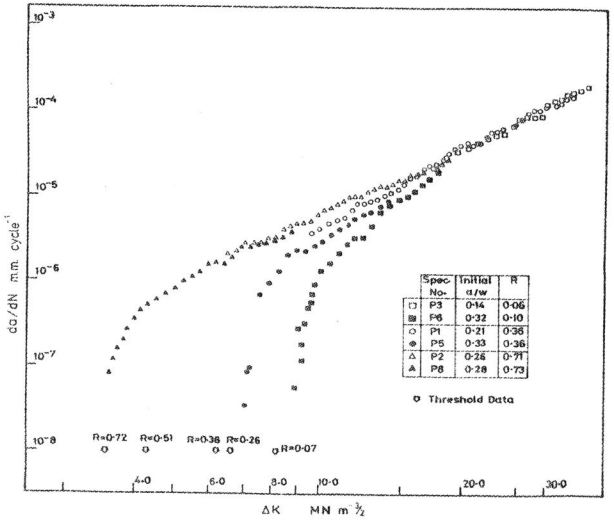

Figure 2 The influence of R ratio (0.06 - 0.73) on the fcg curves of a medium carbon/manganese pearlitic steel tested in laboratory air at a frequency of $\sim$85 Hz.

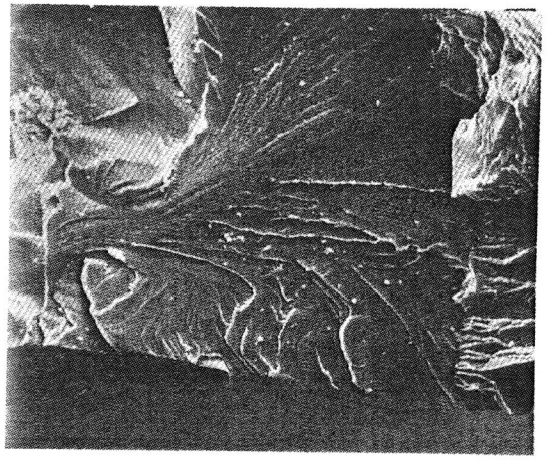

Figure 3 A planar facet formed in a single grain of α-titanium in a specimen tested in laboratory air at a frequency of ~100 Hz. The appropriate ΔK value for this region was ~10 MPa•m$^{1/2}$. Magnification X 200.

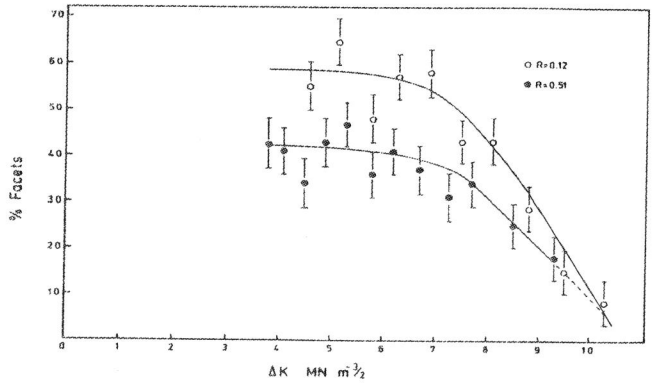

Figure 4 The percentage of fracture face covered by transgranular facets in an α/β Ti 6Al 4V alloy tested in laboratory air as a function of ΔK.

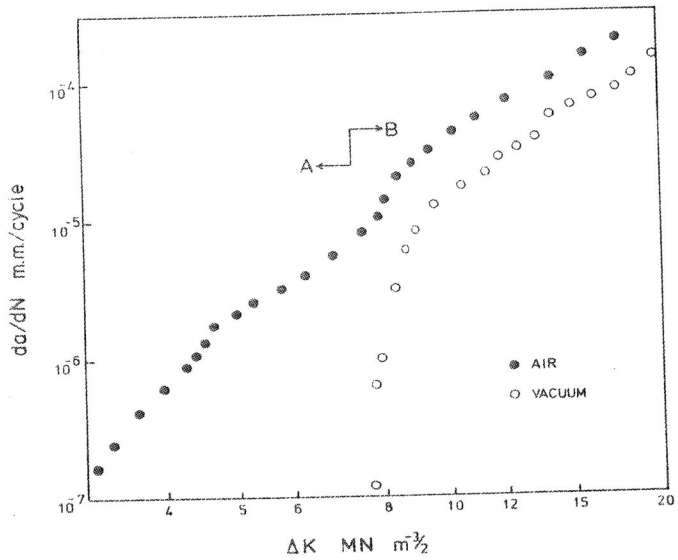

Figure 5 The fcg curves for mill annealed Ti 6Al 4V tested in laboratory air and vacuum (< 3.3 mPa) at R = 0.35.

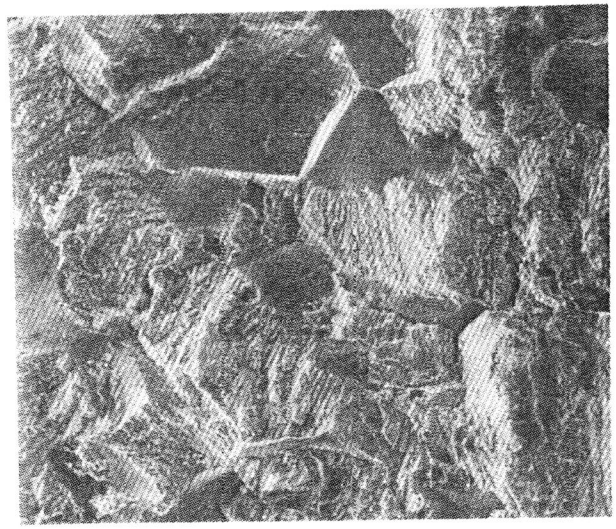

Figure 6 Intergranular separation on the fatigue fracture face of a low carbon mild steel tested in laboratory air. ΔK ~ 10 MPa•m$^{1/2}$. Magnification X 175.

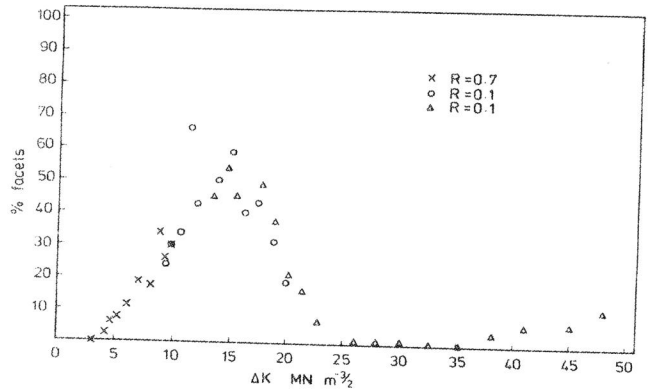

Figure 7 The percentage of fracture face covered by intergranular fracture faces as a function of ΔK for R ratios of 0.7 and 0.1 in an En 24 steel tested in air.

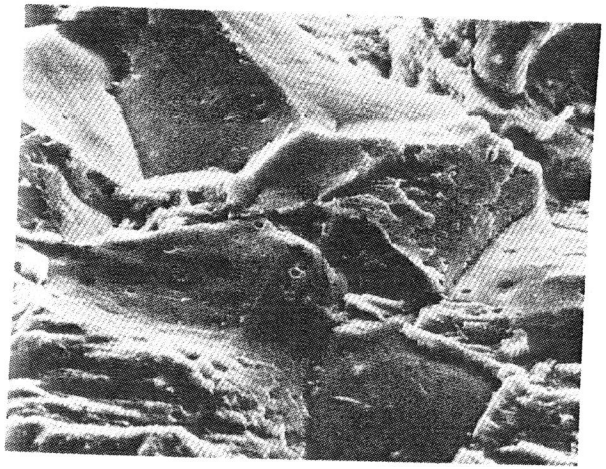

Figure 8 The fracture surface of an En 24 steel showing smooth intergranular facets. Tested in air, R = 0.35, ΔK = ~ 11 MPa•m$^{1/2}$. Magnification X 1700.

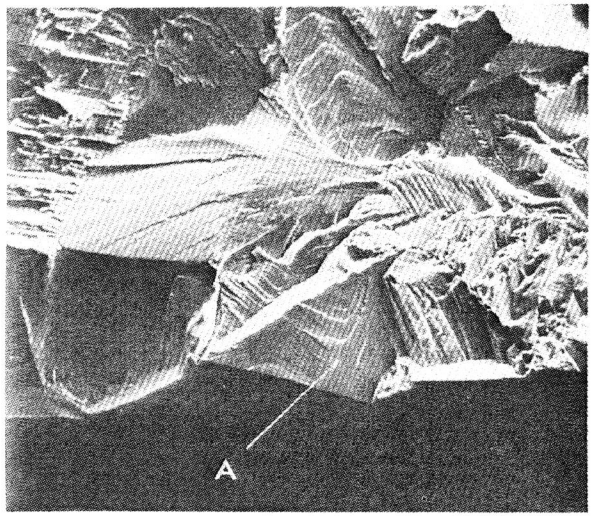

Figure 9 An example of an (0001) facet (A) on the fatigue fracture face of α-titanium tested in laboratory air. Magnification X 200.

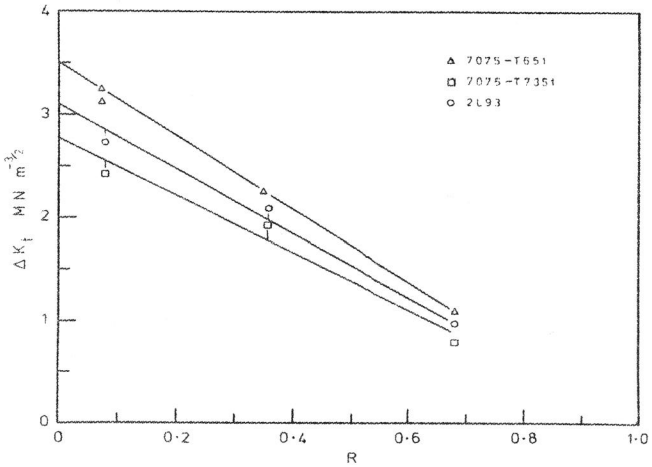

Figure 10 The influence of R ratio on the ΔK threshold level (da/dN < 10^{-8}mm/cycle) for an aluminium/zinc/magnesium alloy (7075) and an aluminium copper alloy (2L93).

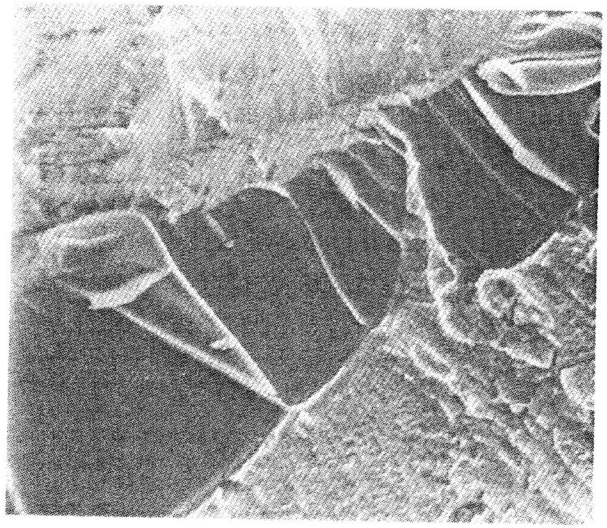

Figure 11 Flat dark shiny faces formed in the threshold region of the 7075-T651 alloy tested in air at R = 0.68. The average growth rate in these flat regions was $\sim 3 \times 10^{-8}$mm/cycle. Magnification X 1,400.

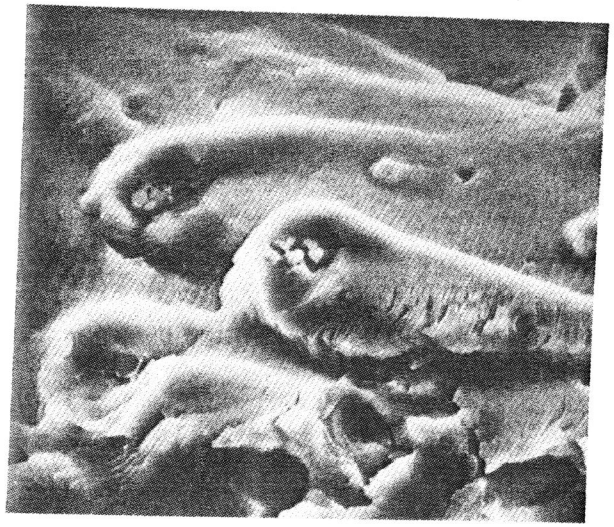

Figure 12 The fatigue fracture surface of an Al/Zn/Mg alloy tested in laboratory air, R = 0.35, $\Delta K \sim 21$ MPa$\cdot$m$^{1/2}$. Magnification X 1,900.

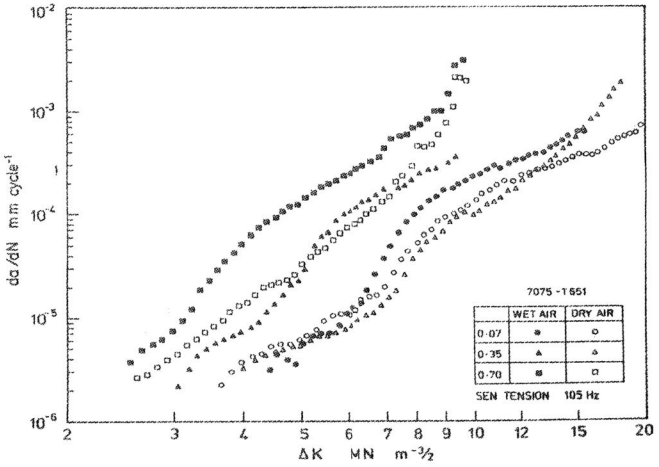

Figure 13 The fcg curves for the aluminium/zinc/magnesium alloy 7075-T651 tested in dry air and wet air at R ratios of 0.07, 0.35 and 0.7.

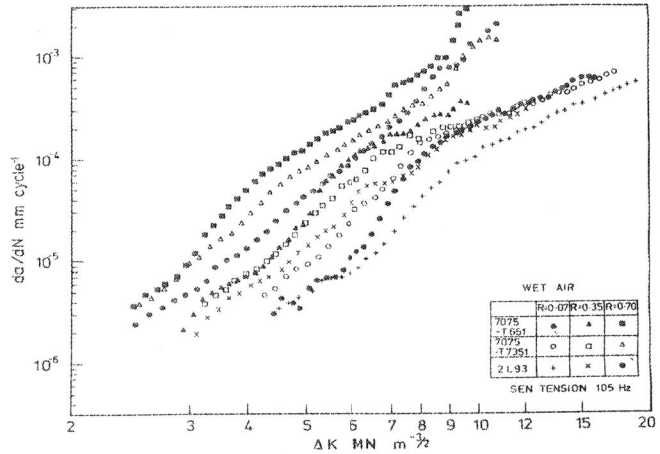

Figure 14 The fcg curves for the aluminium alloys 7075-T651, 7075-T7351 and 2L93 tested in wet air for R ratios 0.07, 0.35 and 0.07.

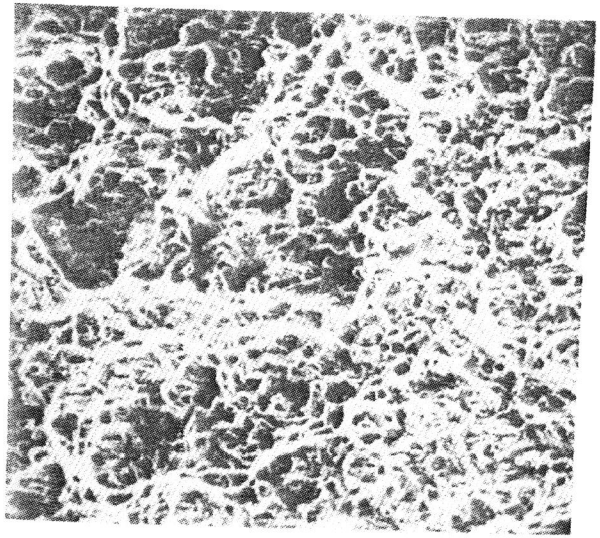

Figure 15 The fatigue fracture surface of a 7075-T651 Al/Zn/Mg alloy tested in wet air at R = 0.35, $\Delta K \sim 18.7$ MPa•m$^{1/2}$. Magnification X 200.

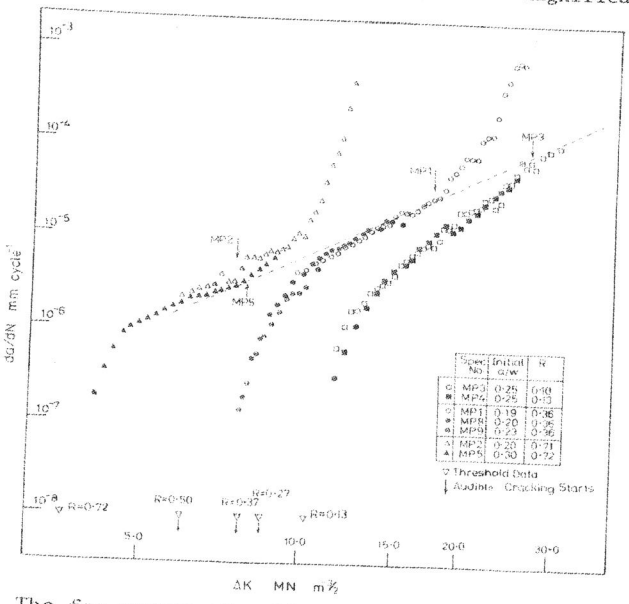

Figure 16 The fcg curves of a C/Mn pearlitic steel containing banded martensite. Tested in laboratory air between R = 0.1 and R = 0.72.

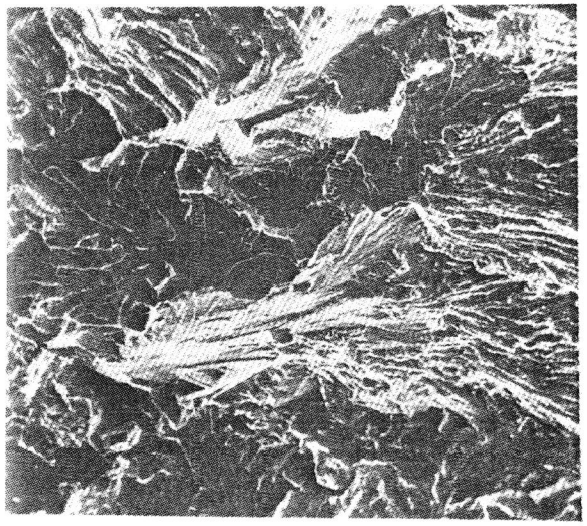

Figure 17 Cleavage facets on the fatigue fractuer surfaces of the C/Mn steel containing banded martensite. R = 0.33, $\Delta K \sim 19.6$ MPa•m$^{1/2}$. Magnification X 420.

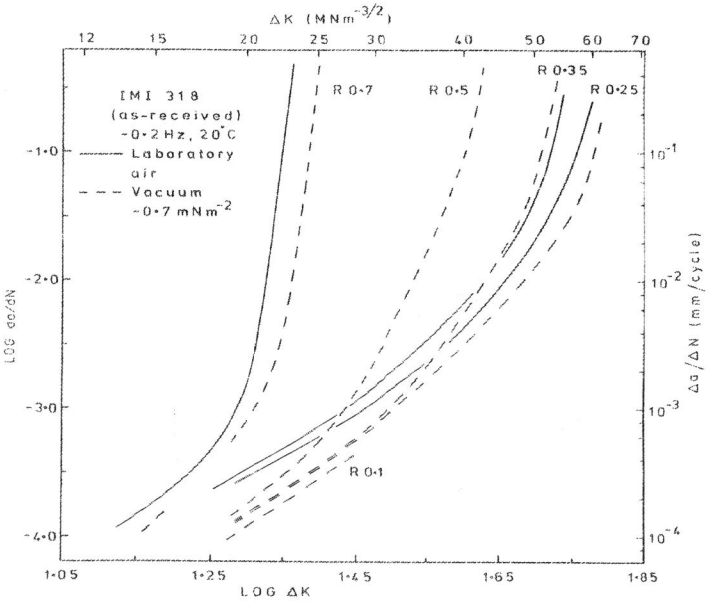

Figure 18 The fcg curves for a Ti 6Al 4V alloy tested in air and vacuum (< 0.7 mPa) at R = 0.7, 0.55, 0.35, 0.25 at a frequency of 0.2 Hz.

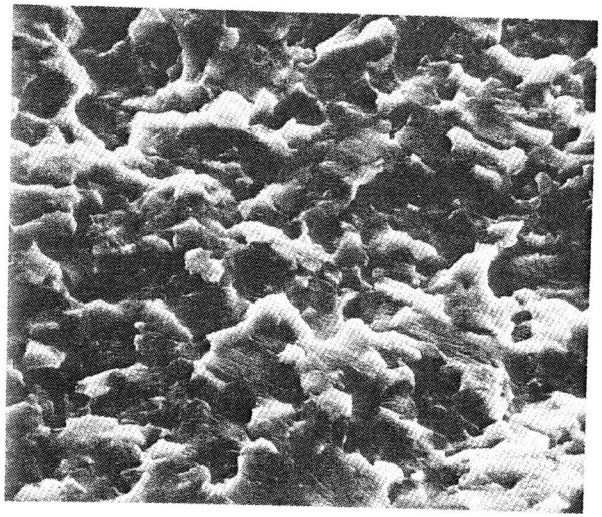

Figure 19 The fatigue fracture surface of a Ti 6Al 4V specimen tested in air at R = 0.25, $\Delta K \sim 19$ MPa. Magnification X 1,660.

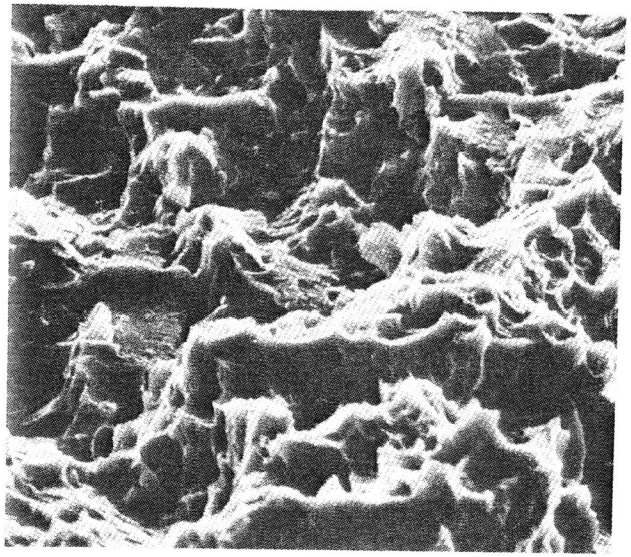

Figure 20 The fracture surface of a Ti 6Al 4V alloy tested under static load conditions in air $K_{max} \sim 48$ MPa$\cdot$m$^{1/2}$. Magnification X 1,600.